ELSEVIER
Available online at www.sciencedirect.com
ScienceDirect
Energy Procedia 4 (2011) 1026–1034
Energy Procedia
www.elsevier.com/locate/procedia

GHGT-10

Thermodynamic Evaluation of Membrane Based Oxyfuel Power Plants with 700°C Technology

Renzo Castillo[1]*

Forschungszentrum Jülich, Institute of Energy Research, IEF-STE: Systems Analysis and Technology Evaluation,52425 Jülich, Germany

Abstract

Cryogenic air separation is the only available state-of-the-art technology for oxyfuel power plants and represents an important burden to the total plant efficiency. Nowadays, high temperature ceramic membranes, which are associated with significantly lower efficiency losses, are foreseen as the best candidate to challenge cryogenics for high tonnage oxygen production for this type of CCS power stations. In this study, two oxyfuel plant designs were developed, the first based on the state-of-the-art supercritical 600 ºC hard coal plant Nordrhein-Westfalen and the second on the advanced ultra-supercritical 700 °C pulverized coal-fired power plant. The membrane-based air separation unit was modeled considering the three-end concept, where oxygen is transported across the membrane aided by a compressor at the feed side and by a vacuum pump at the permeate side. This paper analyzes the influence of both, the cryogenic and high temperature membrane air separation units on the net plant efficiency, considering the same boundary conditions and equivalent thermal integrations. Moreover, the oxygen permeation rate, heat recovery, and required membrane area are also evaluated at different membrane operating conditions.

Keywords: ceramic membranes; MIEC; CCS; oxyfuel; ASU

1. Introduction

The reduction of anthropogenic carbon dioxide emissions resulting from the use of coal is one of the most important challenges in addressing global climate change. Carbon Capture and Storage (CCS) is a technology which captures carbon dioxide from power plants for further storage under the ground. Broadly, three different types of CCS technologies exist: oxyfuel combustion, pre-combustion, and post-combustion. This paper is focused on the oxyfuel combustion concept, where the fuel is burned with pure oxygen instead of air and mixed with a recycled part of the flue gas to maintain the combustion temperature level. Thus, the carbon dioxide concentration in the product flue gas increases dramatically, facilitating its capture. Cryogenic air separation (C-ASU) is the only available state-of-the-art technology for oxyfuel power plants and represents an important burden to the total plant efficiency and compared with conventional air combustion plants, total efficiency drops between 8 and 12

[1*] Corresponding author. Tel.: +49 (0) 2461 61-6556; fax: +49 (0) 2461 61-2540.
E-mail address: r.castillo@fz-juelich.de.

doi:10.1016/j.egypro.2011.01.151

percentage points (%-points) can be expected [1]. Nowadays, high temperature ceramic membranes (HTM), which are associated with significantly lower efficiency losses, are foreseen as the best candidate to challenge cryogenics for high tonnage oxygen production [2]. Because their technical advantages -no sweep gas is required on the permeate side and membrane surfaces remain chemically stable without any contact with the contaminants presented in the flue gas, and conventional flue gas cleaning and materials can be used- this paper is focused on the three-end membrane separation concept. Although this concept can be a good technological option for membrane-based oxyfuel plants in the near future, the advantages of this process with respect to the cryogenic oxygen separation are still unclear for a variety of reasons. First of all, differing plant assumptions were considered in previous thermodynamic analysis found in the literature [3-5]. Secondly, an appropriated study considering the effect of the plant performance on the required membrane area, which represents an important criterion to evaluate the viability of this technology for oxyfuel power plants, is missing. In addition to this carbon-low technology, efficiency improvements in the basic coal power plant concept are required for future power supply in order to master the technological challenge of resource saving, carbon capturing and affordable generation technologies. In the long term, i.e. after 2020, the realization of 700°C power technology, which represents plant efficiencies over 50%, is an important requirement for a successful CCS technology implementation. For these reasons, the purpose of this investigation is to compare the influence of the cryogenic and three-end HTM air separation units on the thermal performance of the oxyfuel power plant considering equivalent thermal integration and boundary conditions, as well as to analyze the impact of the plant operating conditions on the membrane unit design.

2. Oxyfuel power plants

In an oxyfuel process, air has to be treated in an Air Separation Unit (ASU) to take out the oxygen required for combustion. Oxygen purity and recovery (O_2 separation ratio) have important influence on plant performance and depend on the ASU technology applied. The cryogenic and membrane-based oxyfuel power plants presented are based on the advanced supercritical (SC) 600 °C and ultra-supercritical (USC) 700°C coal-fired power plant concepts [6-7], and were modeled using Aspen Plus® process simulation software. Plant performance calculations were done at ISO-conditions (ambient at 15°C, 1.013 bar, and 60% relative humidity) and considering the common characteristics presented in Table 1. The amount of oxygen required were calculated considering coal combustion with 15% of oxygen in excess, whereas the total amount of flue gas recycled to the furnace corresponds to an adiabatic combustion temperature of 2120 °C. Simplified plant arrangement for conventional coal fired plant, as well as for both oxyfuel plants are depicted in Figure 1.

For the SC and USC conventional coal-fired plants (figure 1a), the flue gas exits the boiler at 370°C/380°C[2] and then is denitrified by a hot-side, high-dust selective catalytic reduction (DENOX unit). After that, the flue gas is cooled down to 115°C (above its acid dew point) in an air pre-heater (AIR PRE-HX unit), while the secondary combustion air is heated to 350°C/360°C and a portion of the primary air to 250°C. This arrangement is conceived to reach a dried coal temperature of 100°C after coal-milling. Besides, also part of the hot flue gas energy is integrated into the steam cycle (Q-STEAM). The denitrified flue gas is then further dedusted by a cold side electrostatic precipitator (ESP unit) and finally desulphurized (FGD unit) leaving the plant totally saturated with water at 50°C. Air infiltrations assumed are referred as a portion of the stoichiometric combustion air (13.5% in boiler and 2.5% in the ESP unit) and net plant efficiencies of 45.9% (555 MW) and 50.1% (606 MW) were obtained for the SC 600°C and USC 700°C power plants, respectively.

For the studied oxyfuel processes (figures 1b and 1c), the flue gas exiting the boiler at 370°C/380°C is dedusted by a hot-side electrostatic precipitator (ESP unit) and then denitrified by a hot-side, low-dust selective catalytic reduction (DENOX unit), the presence of air infiltrations in the ESP unit reduces the flue gas temperature to 363°C/373°C. Afterwards, the flue gas is cooled down to 260°C/270°C to heat the primary and secondary recycled flue gas streams via a regenerative gas/gas heat exchanger (HX-GG unit). As in the AIR PRE-HX unit (figure 1a), here also part of the hot flue gas thermal energy is integrated into the steam cycle (Q-STEAM). After that, some of the flue gas thermal energy is recovered by cooling it down to 160°C (above its acid dew point[3] [8]) in the HX-RECOV unit. For the cryogenic oxyfuel process, oxygen is heated from 13°C to 210°C/220°C and also some heat is

[2] First value for SC 600°C technology and second for USC 700°C technology.

[3] Under the studied oxyfuel conditions, the calculated dry SOx concentration in flue gas (after boiler) is around 1660 ppm and according to experimental results presented by Stanger et al. [8], this value represents an acid dew point between 140°C and 150°C.

integrated into the steam cycle (Q-LP1). For the membrane based oxyfuel process, two heat streams are integrated (Q-LP1 and Q-HP1). Subsequently, the dedusted flue gas is separated into two streams: the secondary recycle flue gas which is heated up to 313°C/323°C and sent back to the furnace, and the remaining flue gas which is further quenched to 115°C (QUENCH unit), desulphurized (FGD unit), dehydrated and cooled down to 23 °C (FG COND unit). During the dehydration step, part of the flue gas latent heat (water vapor condensation) is integrated into the steam cycle (Q-LP2 and Q-LP1 for the cryogenic and membrane-based oxyfuel processes, respectively). The cleaned flue gas is then split again into a primary recycled flue gas and a net flue gas. The primary recycled flue gas is heated in the HX-GG unit and sent into the mills to dry and transport the pulverized coal to the burners. The final temperature of the dried coal was set at 100°C. The mass of this recycled stream was assumed to be double that of raw coal. Finally, the net flue gas, which is mainly CO_2 (purity between 75 and 80%), is compressed and purified in the CO2 COMP unit before delivery into a pipeline for further transport and storage. This process is done by condensation and requires changes in the flue gas pressure and temperature to achieve the two-phase region (range between -50°C and 0°C, and 15 bar and 60 bar [9]).

Table 1: Main specifications for supercritical 600°C and ultra-supercritical 700°C power technologies.

Boiler: Supercritical, once through with single reheat	**SC 600°C / USC 700°C**
Coal type and lower heating value:	Kleinkopje, 24991 kJ/kg
Coal composition by weight (C, H, N, O, S, Ash, H_2O)	(65.5%, 3.53%, 1.49%, 7.42%, 0.59%, 14.12%, 7.3%)
Coal consumption:	48.42 kg/s
Thermal capacity:	1210 MW_{th}
Boiler efficiency:	95%
Average furnace temperature:	1200°C / 1250°C
Lambda (oxygen excess):	1.15
High pressure steam (temp. and pressure):	600°C, 285 bar / 705°C, 365 bar
Intermediate pressure steam (temp. and pressure):	620°C, 60 bar / 720°C, 67 bar
Flue gas temperature after boiler:	370°C / 380°C
Steam cycle and cooling tower:	**SC 600°C / USC 700°C**
Turbine expansions, and isentropic and mechanical efficiencies:	
High pressure turbine (HP-T)	from 285 to 66 bar, 93%, 99% / from 365 to 73 bar, 94%, 99%
Intermediate pressure turbine (IP-T)	from 60 to 5.5 bar, 95%, 99% / from 67 to 5.5 bar, 96%, 99%
Low pressure turbine (LP-T)	from 5.5 to 0.045 bar, 90%, 99% / from 5.5 to 0.045 bar, 91%, 99%
Pressure profile of steam extractions:	(HP: 89, 66; IP: 26.5, 11.9, 5.5; LP: 3.0, 1.5, 0.35) bar / (HP: 120, 90; IP: 35.25, 14.35, 5.5; LP: 3.5, 2, 0.8, 0.2) bar
Steam extractions pressure drop:	5%
Condenser pressure and saturation temperature:	45 mbar, 31°C
Condensate temperature:	30°C
Pre-heaters for HP feed water and LP condensate:	3HP, 1 feed water tank, 4LP / 3HP, 1 feed water tank, 5LP
Feed water tank pressure and saturation temperature:	11.3 bar, 185.3°C / 13.6 bar, 193.7°C
Boiler feed water conditions (temperature and pressure):	303.4°C, 327 bar / 330°C, 407 bar
Feed water and condensate pumps:	Electrically driven
Cooling tower type:	Natural draft
Cooling water temperature:	13°C
Heated air conditions (temperature and humidity):	25°C, 100% saturated
Cycles of concentration[a]:	3

[a] Ratio between make-up rate and bleed rate.

2.1 Cryogenic oxyfuel plant

The oxygen required by this plant is separated by condensation at low temperatures throughout a multi-stage distillation. Detailed information about this process can be found in [10-11]. The energy consumption increases with higher O_2 purity requirements, and although the higher the O_2 purity, the lower the energy required by the CO_2 compression and purification step, previous studies have demonstrated that 95% purity is an optimum value, because further O_2 purification requires more energy than the savings obtained during the carbon dioxide compression [12]. In this investigation, the C-ASU process was modeled as a black box assuming a 95% purity of produced O_2 containing 3.8% Ar and 1.2% N_2 [1], and an oxygen separation efficiency of 97.72% [12]. The produced oxygen (103.2 kg/s) at 13°C and 1.1 bar is pre-heated by the flue gas and then mixed with the secondary recycled flue gas before entering into the furnace (see figure 1b). Based on information presented by Darde et al. [13] for a state-of-the-art technology and future developments, specific energy consumptions of 200 and 160 kWh/tonO_2 were assumed for the cryogenic ASU with 600°C and 700°C technologies, respectively. Net plant efficiencies of 36.4% (SC 600°C) and 39.9% (USC 700°C) were obtained for these oxyfuel power plants.

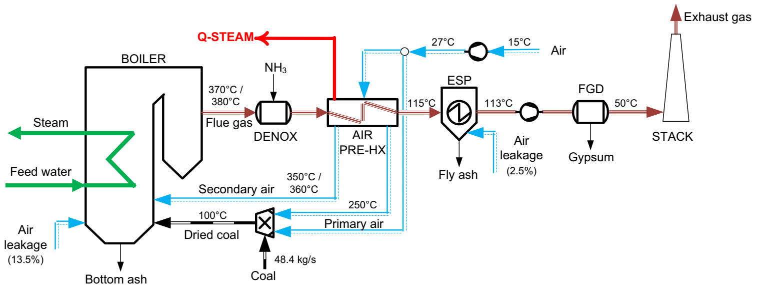

Figure 1a: Conventional coal-fired power plant process

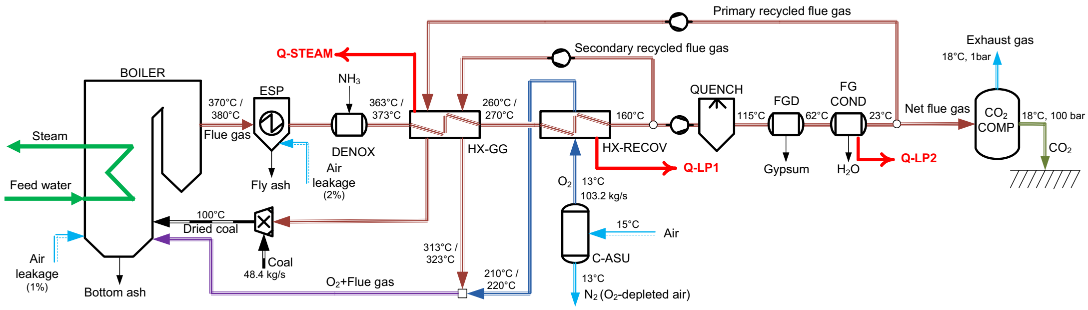

Figure 1b: Cryogenic oxyfuel process

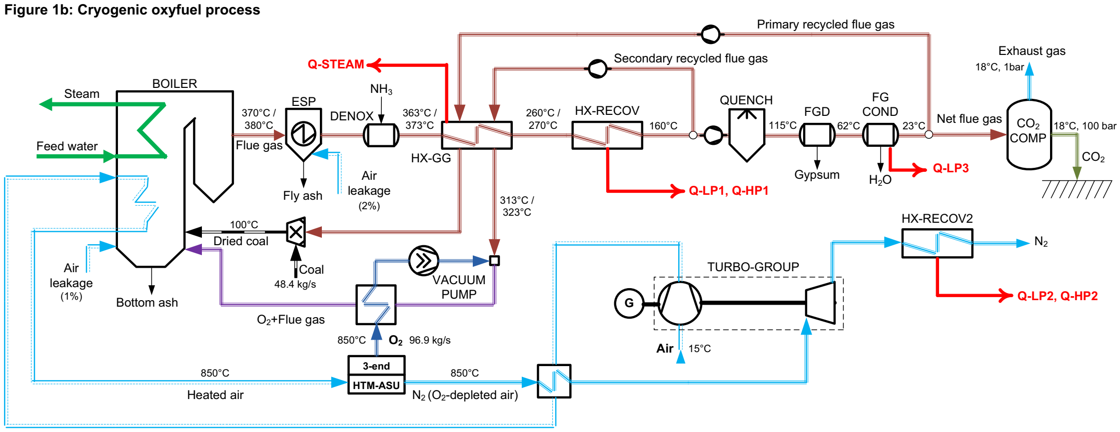

Figure 1c: Membrane-based oxyfuel process

Figure 1: Process flow diagrams of conventional and oxyfuel power stations modeled (air and flue gas paths).

2.2 Membrane-based oxyfuel plant

High temperature membranes for oxygen production are based on ceramic materials and are in the development stage [14]. These membranes, also known as Mixed Ionic Electronic Conducting (MIEC) membranes, operate at temperatures above 700°C to conduct ionized oxygen throughout the material with a selectivity of 100% [15]. In the three-end concept, no sweep gas is used on the permeate side, and to generate the O_2-partial pressure difference, pressurized air is conducted to the feed side, whereas the permeate side is set at vacuum conditions. In the plant model developed (see figure 1c), atmospheric air is compressed and then heated into the boiler up to 850°C (assumed membrane operation temperature) before being supplied to the membrane. Afterwards, the pure O_2 separated from the air (96.9 kg/s on the permeate side) is led to the furnace by a vacuum pump to enrich the secondary recycled flue gas with oxygen before combustion. A heat exchanger is used to heat the O_2-enriched secondary recycled flue gas, cooling the produced high-temperature oxygen before entering into the vacuum pump. The oxygen-depleted air (mainly N_2), which leaves the membrane at high pressure and temperature (retentate), is then expanded in a turbine to drive the air compressor and to generate additional electrical power. Air compressor and turbine together are called as turbo-group. Since the oxygen supplied to the furnace should be constant, the air required by the plant depends on the membrane's ability to separate oxygen. Turbo-group and vacuum pump serve directly to the membrane module and determine the required air mass flow and separation conditions at the feed and permeate sides. These auxiliary components have relevant influence on the global plant performance, so it is important to define some membrane parameters to analyze the oxygen separation process in relation to the turbo-group and vacuum pump energy requirements, and to identify their best operation conditions (see figure 2).

a) Oxygen separation ratio (SR_O_2): This parameter indicates which portion of the incoming oxygen mass is separated by the membrane module. The higher this parameter, the lower the required mass flow of air, and the higher the thermal energy given to the water-steam cycle in the boiler.

b) Turbo-group compression ratio (β): This parameter is the same as the compressor pressure ratio and defines the pressure of the air fed into the membrane (P_{feed}). In conjunction with the SR_O_2, defines the turbo-group energy requirements and the energy content of the depleted off-gas leaving the air turbine (N_2 stream).

c) Retentate oxygen partial pressure ratio (Π_{ret}): This value corresponds to the oxygen partial pressure ratio at the end of the membrane separation process, i.e. retentate (Π_{ret}) and represents the minimum oxygen pressure ratio along the membrane and define the required vacuum ($PO_{2,perm}$). Other parameter that can be used instead of Π_{ret} is the total membrane oxygen partial pressure ratio Π_{memb}, which can be calculated as simple average between feed Π_{feed} and retentate Π_{ret} values if linear oxygen partial pressure distribution along membrane is considered.

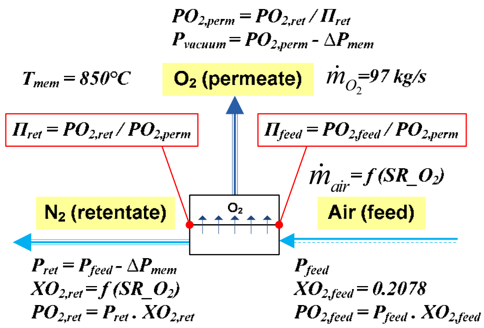

Figure 2: Three-end membrane parameters.

The energy required by the vacuum pump (in MW) was calculated following the equation presented by [16], which is based on the manufacturer's technical information. The separated oxygen mass flow is expressed in kg/s and the required vacuum pressure P_{vacuum} in mbar.

$$\dot{W}_{vacuum} = 23.168 \cdot \dot{m}_{O_2} \cdot P_{vacuum}^{-0.8151} \tag{1}$$

3. Membrane area

Air demand, oxygen partial pressure ratio along the membrane, material used and the operating temperature have a great influence in the required membrane area. Assuming that single phase bulk diffusion limits the oxygen flux through the MIEC membrane, the oxygen permeation rate (JO_2) can be described by the Wagner equation [14] and adapted to express the oxygen flux in function of characterized material constants C_{Wagner} and k_{Wagner} [17]:

$$JO_2(x) = C_{wagner} \cdot e^{-\frac{k_{Wagner}}{T_{memb}}} \cdot \frac{T_{memb}}{d_{memb}} \cdot \ln\left(\frac{PO_2(x)}{PO_{2,perm}}\right) \tag{2}$$

Adopting a shell-and-tube configuration for the membrane module [18], and assuming a linear oxygen partial pressure distribution along the membrane ($PO_2(x)$), a mathematical integration of the modified Wagner equation ($\dot{m}_{O_2} = \int JO_2 \cdot dA$) was performed to calculate the required membrane area:

$$A = \frac{\dot{m}_{O_2} \cdot \left(C_{wagner} \cdot e^{-\frac{k_{Wagner}}{T_{memb}}} \cdot \frac{T_{memb}}{d_{memb}} \right)^{-1}}{\ln\left(\frac{\Pi_{ret}}{e}\right) + \left(\frac{1-\left(XO_{2,feed} \cdot SR\_O_2\right)}{\left(1-XO_{2,feed}\right) \cdot SR\_O_2} \right) \cdot \ln\left(\frac{1-\left(XO_{2,feed} \cdot SR\_O_2\right)}{1-SR\_O_2} \right)} \tag{3}$$

Equation 3 shows that aside from material properties and operating temperature, the required membrane area depends only on the oxygen recovery and Π_{ret}, but not on the turbo-group compression ratio β. Because of their high ionic and electronic conductivity, perovskite-type (ABO_3) ceramic membranes present the highest oxygen permeability as compared to other MIEC membranes [2, 15]. In this study, perovskite $Ba_{0.5}Sr_{0.5}CO_{0.8}Fe_{0.2}O_{3-\delta}$ (BSCF) was selected as membrane material with C_{Wagner}=1.004 x 10^{-8} mol/(cm.s.K) and k_{Wagner}= 6201K obtained from experimental characterization [17]. Moreover, a membrane thickness d_{memb} and temperature T_{memb} of 0.6 mm and 850°C were assumed, respectively. Figure 3 depicts the calculated membrane area required to separate 96.9 kg/s of oxygen and the average oxygen permeation rate JO_2. The situation is most beneficial with respect to the membrane area in cases where the oxygen recovery SR_O_2 is high, and also where Π_{ret} is high. It is because in the first case $PO_{2,ret}$ decreases as more oxygen is recovered, making more vacuum necessary on the permeate side to keep Π_{ret} constant ($PO_{2,perm}$ decreases and Π_{feed} increases). In the same way, for the second case more vacuum is also required at higher Π_{ret} values, improving the oxygen partial pressure ratio along the membrane and the oxygen permeation rate as well (see equation 2).

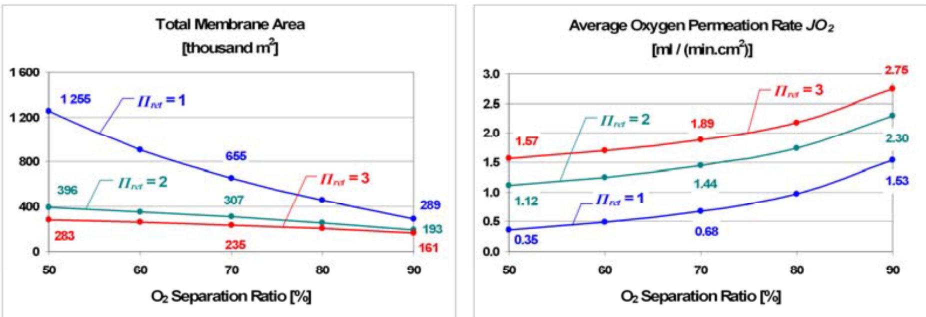

(a) (b)

Figure 3: (a) total membrane area required and (b) average oxygen permeation rate.

4. Thermal integration

In contrast to the thermal energy that can be recovered from the flue gas, which is constant, the energy that can be integrated from the O_2-depleted air in membrane-based plants depends on the membrane and turbo-group parameters and is promoted at low SR_O_2 ratios (high O_2-depleted air flow) and high β values (high temperature after turbine expansion). When high amounts of energy are integrated into the water/steam cycle, less steam extractions are required to pre-heat condensate and feed water, changing the steam cycle configuration (reduction of condensate and feed water pre-heaters). Table 2 presents the temperature profile of cold (LP condensate or HP feed water) and hot (flue gas or O_2-depleted air) streams for each integrated heat flux. The minimum temperature difference assumed between hot and cold streams for a gas-liquid heat exchanger is 10K.

Table 2: Thermal integration: Temperature profile of hot and cold streams.

		Membrane-Based Oxyfuel (HTM-ASU)						Cryogenic Oxyfuel (C-ASU)	
		SC 600°C / USC 700°C						SC 600°C / USC 700°C	
		Q-STEAM	Q-HP1	Q-LP1	Q-HP2	Q-LP2	Q-LP3	Q-LP1	Q-LP2
ΔT Hot stream (°C)	from:	363 / 373	260 / 270	202 / 212	>300	202 / 212	63	220 / 230	63
	to:	260 / 270	202 / 212	160	202 / 212	>40	>40	160	>40
ΔT Cold stream (°C)	from:	30	192 / 202	30	192 / 202	30	30	30	30
	to:	185 / 193	250 / 260	185 / 193	303 / 330	185 / 193	53	185 / 193	53

At low SR_O_2 values, the amount of heat that can be recovered is so high that it cannot be entirely integrated without changing the inlet feed water temperature in the boiler (303.4°C/330°C). Thus, to keep this temperature constant, only part of the N_2 stream energy is integrated, leaving the HX-RECOV2 at temperatures above the limit of 40°C. As the SR_O_2 increases, the available thermal heat from N_2 stream decreases (less N_2 mass flow) and the boiler feed water mass flow increases, so higher portions of the available thermal energy from N_2 can be integrated into the steam cycle (exiting N_2 temperature after HX-RECOV2 unit decreases). Figure 4a depicts for a particular membrane-based oxyfuel plant the reduction of the total integrated heat as the SR_O_2 increases. In general, the achieved gross plant power -from steam (W_STURB) and turbo-group (W_TGROUP) cycles- increases as the SR_O_2 increases because the better thermal integration (see figure 4b). But, although that, the vacuum pump power required also increases noticeably while the power consumed by other plant components stay relatively constant, so the net power reach a maximum value and then decreases (see figure 4c).

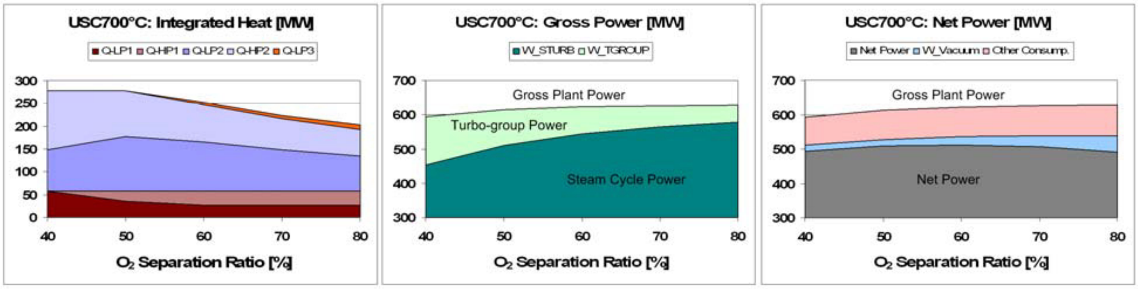

(a) (b) (c)

Figure 4: Membrane-based oxyfuel plant with USC 700°C technology (β=10 and Π_{ret}=3): (a) Heat integrated into the steam cycle, (b) gross power, and (c) net power.

Figure 5 shows the calculated net plant efficiencies in relation to β and SR_O_2 considering different fixed Π_{ret} and Π_{memb} values. Here it is also possible to appreciate the increasing-decreasing tendency of the net efficiency. Curves β =6.9 and β =10 have similar behaviour due to in these cases internal turbo-group regeneration is performed while for β = 15 not. Additionally, as Π_{ret} and Π_{memb} increases more vacuum power is required resulting in a net plant efficiency reduction, but also less membrane area is required.

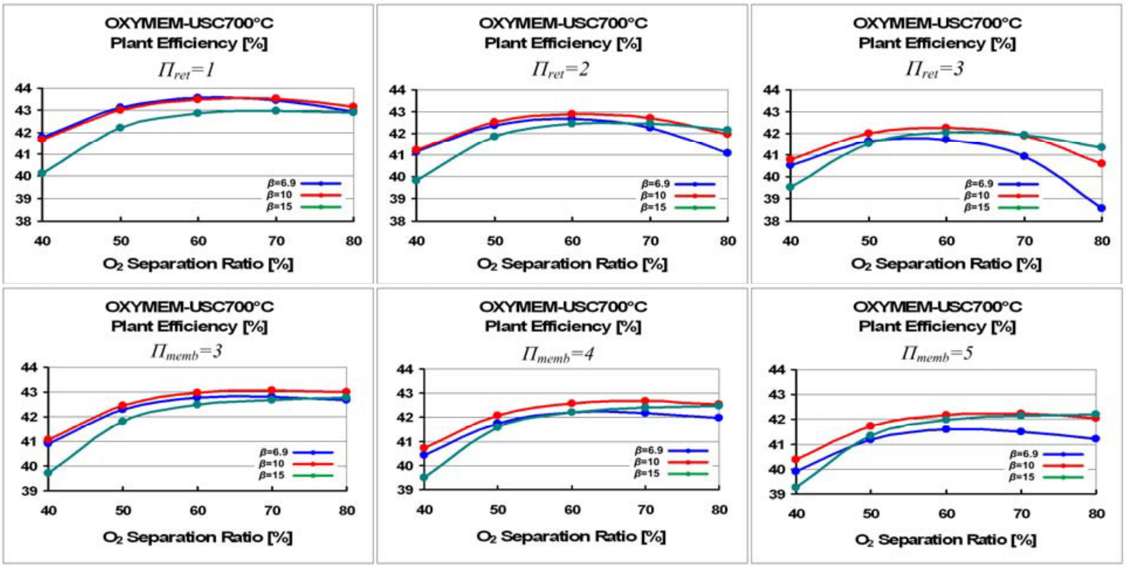

Figure 5: Net plant efficiency of membrane-based oxyfuel plant with USC 700°C technology for different Π_{ret} (first row) and Π_{memb} (second row).

In the depicted cases where Π_{memb} is constant and equal to 3, 4 and 5 (second row), the required membrane area is also constant and equal to 376, 296 and 254 thousand m^2, respectively. For the HTM oxyfuel concept with USC 700°C power technology, the maximum efficiency is reached by β =10 and around SR_O_2=60%, thus considering a relative low membrane area requirement with an acceptable plant efficiency, the case where Π_{memb} =5 (Π_{ret} =3.12) was selected as best option for this power technology (net efficiency 42.2%). For power technology comparison, the same membrane operating conditions were selected for the membrane-based SC 600°C oxyfuel plant, obtaining a net efficiency of 39.6%. Table 3 summarizes the main performance data of the plants investigated.

Table 3: Performance data of reference and oxyfuel plants with SC 600°C and USC 700°C power technologies.

	Reference Plant		Cryogenic Oxyfuel (C-ASU)		Membrane-Based Oxyfuel (HTM-ASU)	
	SC 600°C	USC 700°C	SC 600°C	USC 700°C	SC 600°C	USC 700°C
Steam cycle output (MW)	604.9	658.2	608.7	639.9	510.5	543.3
Turbo-group net output (MW)	-	-	-	-	79.1	79.1
Plant gross output (MW)	604.1	658.2	608.7	639.9	589.6	622.4
Vacuum pump load (MW)	-	-	-	-	24.8	24.8
Cryogenic ASU load (MW)	-	-	74.1	59.5	-	-
CO_2 compression load (MW)	-	-	54.5	53.6	52.3	51.3
Steam cycle pumps load (MW)	20.1	23.6	20.3	24.2	14.5	16.8
Cooling tower pumps load (MW)	2.6	1.7	2.1	2.0	2.0	1.9
Coal mill load (MW)	1.9	1.9	1.9	1.9	1.9	1.9
Flue gas blower load (MW)	4.8	4.8	0.8	0.8	0.7	0.7
Recirculation blowers load (MW)	-	-	0.8	0.8	0.9	0.9
Air blower load (MW)	6.1	6.1	-	-	-	-
Other aux. equipment load (MW)	2.1	2.1	2.1	2.1	2.1	2.1
Total equipment load (MW)	38.4	40.2	156.6	144.9	99.2	100.4
Heat losses in generator (MWth)	11.2	12.1	11.2	11.8	10.9	11.5
Plant net output (MW)	555.3	605.9	440.9	483.2	479.5	510.5
Net plant efficiency LHV (%)	45.9	50.1	36.4	39.9	39.6	42.2
Efficiency drop (%-points)	-	-	9.5	10.2	6.3	7.9
Specific coal consumption (g/kWh)	313.8	287.7	395.3	360.7	363.5	341.5
Total integrated heat (MW_{th})	10.2	19.4	58.1	58.5	251.9	253.4
Final O_2-deplated air temperature (°C)	-	-	-	-	40	40
Boiler feed water rate (kg/s)	431.0	398.7	427.8	406.7	302.2	281.1
Cooling tower released heat (MW_{th})	560.9	510.2	813.0	771.3	749.7	718.2
Circulating cooling water (kg/s)	245.5	220.7	351.5	332.9	323.2	309.1
Draw-off cooling water (kg/s)	81.8	73.6	117.2	111.0	107.7	103.0
Flue gas rate after combustion (kg/s)	575.8	575.8	459.4	461.6	478.4	479.2
Net flue gas rate (kg/s)	596.6	596.6	139.6	140.1	134.1	134.1
Recycle rate (%)	-	-	66.4	66.5	69	69
Air feed rate (kg/s)	473.2	473.2	432.1	432.1	700.4	700.4
Oxygen flow rate (kg/s)	-	-	103.2	103.2	96.9	96.9
Oxygen purity (%)	-	-	95	95	100	100
Oxygen separation ratio (%)	-	-	97.7	97.7	60.0	60.0
Retentate O_2 partial pressure ratio	-	-	-	-	3.12	3.12
Membrane O_2 partial pressure ratio	-	-	-	-	5.0	5.0
O_2 permeation rate (ml/(min.cm^2))	-	-	-	-	1.75	1.75
Membrane area (thousand m^2)	-	-	-	-	254	254
Specific membrane area (m^2/kW$_{el}$)	-	-	-	-	0.530	0.497
Captured CO_2 rate (kg/s)	-	-	108.6	108.6	108.1	108.1
CO_2 recovery rate (%)	-	-	90.2	90.2	90.1	90.0
CO_2 compression work (kWh/tonCO_2)[a]	-	-	139.4	137.1	134.3	131.9
Captured CO_2 composition:						
CO_2 (mol %)	-	-	95.01	95.08	95.09	95.09
O_2 (mol %)	-	-	1.60	1.68	2.03	2.03
N_2 (mol %)	-	-	2.17	2.06	2.81	2.81
Ar (mol %)	-	-	1.2	1.16	0.05	0.05
Exhaust gas flow rate (kg/s)	596.6	596.6	29.3	29.8	24.3	24.4
CO_2 emissions (kg/s)	116.9	116.9	11.4	11.3	11.5	11.5
Specific CO_2 emissions (g/kWh)	757.7	694.6	93.1	84.2	86.3	81.5
Contaminants in flue gas after boiler / after cleaning:						
SOx (mg/Nm^3)	1323 / 150	1323/150	4323 / 150	4320 / 150	4428 / 150	4424 / 150
NOx (mg/Nm^3)	680 / 100	865/100	229 / 100	314 / 100	240 / 100	306 / 100

[a] Referred to the purified CO_2 stream

5. Conclusions

Considering the HTM-ASU oxyfuel concept, net efficiencies of 39.6% and 42.2% can be reached with SC600°C and USC700°C power technologies, respectively. These values are considerably higher than the corresponding 36.4% and 39.9% reached when the C-ASU oxyfuel concept is applied. To make it possible, heat recovery from flue gas and N_2 streams is essential, because more than 20% of the coal energy input must be integrated into the steam cycle (≈250 MW_{th}). Besides, 254 000 m^2 of membrane area is required (O_2 permeation rate of 1.75 ml/(min.cm^2)).

It is thermodynamically more desirable to operate the HTM parameters at: $50\% < SR\_O_2 < 70\%$, $2 < \Pi_{ret} < 3$ and $\beta = 10$, because high net plant efficiencies between 42% and 43% can be reached using USC 700°C technology. It means, between 2 and 3 %-points over the C-ASU oxyfuel plant efficiency (39.9%).

Although the oxygen permeation rates reached for this type of oxyfuel plant (between 1 and 3 ml/(min.cm^2)) are considerably lower than the value presented by [19] as the minimum required for economic viability of this technology (10 ml/(min.cm^2)), further improvements in process design, membrane material and manufacturing, as well as external factors such as CO_2 penalties, and energy legislation are still necessary to make this breakthrough technology realizable. Finally, techno-economic and environmental assessments are still necessary for a complete comparison between these oxyfuel technologies.

Acknowledgments

Financial support from the Helmholtz Association of German Research Centers (Initiative and Networking Fund) through the Helmholtz Alliance MEM-BRAIN is gratefully acknowledged.

References

[1] A. Kather and S. Gunter. The oxycoal process with cryogenic oxygen supply Naturwissenschaften 2009; 96(9): 1-18.
[2] M. Betz. Ceramic Membranes for Oxyfuel Power Plants. In: Fourth International Conference on Clean Coal Technologies 2009: Dresden, Germany, 18-21 May.
[3] I. Pfaff and A. Kather. Comparative thermodynamic analysis and integration issues of CCS steam power plants based on oxy-combustion with cryogenic or membrane based air separation. Energy Procedia 2009; 01: 495-502.
[4] F. Beggel, S. Engels, M. Modigell, et al. Oxyfuel combustion by means of high temperature membranes for air separation. In: Fourth International Conference on Clean Coal Technologies 2009: Dresden, Germany, 18-21 May.
[5] H. Stadler, F. Beggel, M. Habermehl, et al. Oxyfuel coal combustion by efficient integration of oxygen transport membranes. International Journal of Greenhouse Gas Control 2010; In Press, Corrected Proof.
[6] VGB-PowerTech e.V. (ed). Konzeptstudie Referenzkraftwerk Nordrhein-Westfallen (RKW NRW) 2004. Report 85.65.69-T-138, 123, VGB PowerTech service GmbH: Essen, February.
[7] R. Blum, J. Bugge and S. Kjaer. USC 700°C Power Technology - A European Suceess Story -. VGB Power Tech 2009; (4/2009): 26-32.
[8] R. Stanger and T. Wall. Sulphur impacts during pulverised coal combustion in oxy-fuel technology for carbon capture and storage. Progress in Energy and Combustion Science 2010; In Press, Corrected Proof.
[9] R. Castillo. Technical evaluation of CO_2 compression and purification in CCS power plants. In: Fourth International Conference on Clean Coal Technologies 2009: Dresden, Germany, 18-21 May.
[10] W. F. Castle. Air separation and liquefaction: recent developments and prospects for the beginning of the new millennium. International Journal of Refrigeration 2002; 25(1): 158-172.
[11] H. Hausen and H. Linde. Tieftemperaturtechnik : Erzeugung sehr tiefer Temperaturen, Gasverflüssigung u. Zerlegung von Gasgemischen. Second ed., Springer, Berlin, 1985, pp. 597.
[12] D. J. Dillon, V. White, R. J. Allam, et al. Oxy Combustion Processes for CO_2 Capture from Power Plants 2005. IEA Greenhouse Gas R&D Programme and Mitsui Babcock, Report 2005/9, July.
[13] A. Darde, R. Prabhakar, J. P. Tranier, et al. Air separation and flue gas compression and purification units for oxy-coal combustion systems. Energy Procedia 2009; 1(1): 527-534.
[14] J. Sunarso, S. Liu, Y. S. Lin, et al. Oxygen permeation performance of $BaBiO_{3-\delta}$ ceramic membranes. Journal of Membrane Science 2009; 344(1-2): 281-287.
[15] J. H. Park, J. P. Kim and S. H. Son. Oxygen permeation and stability of $Ba_{0.5}Sr_{0.5}Co_{0.8}Fe_{0.2}O_{3-\delta}$ membrane according to trace elements and oxygen partial pressure in synthetic air. Energy Procedia 2009; 1(1): 369-374.
[16] N. Nauels. Technische Analyse von OXYCOAL-AC Kraftwerken mit Aspen Plus unter besonderer Berücksichtigung der Integration der Hochtemperatur-Luftzerlegung mittels Membranen. Diploma Thesis, pp.115. In: Mechanische Verfahrenstechnik, RWTH Aachen University. Aachen, Germany, April 2009.
[17] S. Engels, F. Beggel, M. Modigell, et al. Simulation of a membrane unit for oxyfuel power plants under consideration of realistic BSCF membrane properties. Journal of Membrane Science 2010; In Press, Corrected Proof.
[18] E. Yantovski, J. Gorski, B. Smyth, et al. Zero-emission fuel-fired power plants with ion transport membrane. Energy 2004; 29(12-15): 2077-2088.
[19] R. Bredesen, K. Jordal and A. Bolland. High-temperature membranes in power generation with CO_2 capture. Chemical engineering and processing 2004; 43(9): 1129-1158.